Mapping the Interfacial Binding Surface of Human Secretory Group IIa Phospholipase A_2[†]

Yana Snitko,[‡] Rao S. Koduri,[§] Sang K. Han,[‡] Roohaida Othman,[∥] Sharon F. Baker,[∥] Barbara J. Molini,[§] David C. Wilton,[∥] Michael H. Gelb,*[,§] and Wonhwa Cho*[,‡]

Department of Chemistry (M/C 111), University of Illinois at Chicago, 845 West Taylor Street, Chicago, Illinois 60607-7061, Departments of Chemistry and Biochemistry, University of Washington, Box 351700, Seattle, Washington 98195, and Department of Biochemistry, University of Southampton, Bassett Crescent East, Southampton S09 3TU, U.K.

Received May 21, 1997; Revised Manuscript Received August 13, 1997[⊗]

ABSTRACT: Human secretory group IIa phospholipase A_2 (hIIa-PLA_2) contains a large number of prominent cationic patches on its molecular surface and has exceptionally high affinity for anionic surfaces, including anionic membranes. To identify the cationic amino acid residues that support binding of hIIa-PLA_2 to anionic membranes, we have performed extensive site-directed mutagenesis of this protein and measured vesicle binding and interfacial kinetic properties of the mutants using polymerized liposomes and nonpolymerized anionic vesicles. Unlike other secretory PLA_2s, which have a few cationic residues that support binding of enzyme to anionic membranes, interfacial binding of hIIa-PLA_2 is driven in part by electrostatic interactions involving a number of cationic residues forming patches on the putative interfacial binding surface. Among these residues, the amino-terminal patch composed of Arg-7, Lys-10, and Lys-16 makes the most significant contribution to interfacial adsorption, and this is supplemented by contributions from other patches, most notably Lys-74/Lys-87/Arg-92 and Lys-124/Arg-127. For these mutants, complete vesicle binding occurs in the presence of high vesicle concentrations, and under these conditions the mutants display specific activities comparable to that of wild-type enzyme. These studies indicate that electrostatic interactions between surface lysine and arginine residues and the interface contribute to interfacial binding of hIIa-PLA_2 to anionic vesicles and that cationic residues closest to the opening of the active-site slot make the most important interactions with the membrane. However, because the wild type binds extremely tightly to anionic vesicles, it was not possible to exactly determine what fraction of the total interfacial binding energy is due to electrostatics.

Phospholipases A_2 (PLA_2; E.C. 3.1.1.4)[1] catalyze the hydrolysis of the fatty acid ester at the *sn*-2 position of phospholipids and are found both in intracellular and secreted forms (Dennis, 1994; Kudo et al., 1993; Mayer & Marshall, 1993; Scott & Sigler, 1994). Secretory PLA_2s are small proteins (14−16 kDa) that can be classified into at least five groups based on structural differences (Davidson & Dennis, 1990; Dennis, 1997; Heinrikson et al., 1977). In particular, structures and functions of three major classes of homologous secretory enzymes (classes I, II, and III) have been extensively studied. Since PLA_2 acts on phospholipids in membranes or in other aggregated forms, the reaction cycle includes the interfacial binding which is distinct from the binding of a phospholipid molecule to the active site (Gelb et al., 1995). Fluorometric, crystallographic, and NMR analyses of multiple secretory PLA_2s have led to the proposal of a common interfacial binding surface (IBS) that is located on a flat external surface that surrounds the active-site slot (Peters et al., 1992; Ramirez & Jain; 1991, Scott & Sigler, 1994). A substrate molecule must leave the membrane to travel into the active-site slot to reach the catalytic residues. The putative IBS contains a ring of cationic and hydrophobic residues. A reasonable hypothesis is that cationic residues on the IBS of secretory PLA_2s allow them to bind much more tightly to anionic interfaces than to electrically neutral ones (Ramirez & Jain, 1991). Recent structure−function studies on class I bovine pancreatic PLA_2 (Dua et al., 1995) and class II *Agkistrodon piscivorus piscivorus* PLA_2 (Han et al., 1997) have shown that the binding of these secretory PLA_2s to anionic interfaces is driven in part by electrostatic interactions between anionic membrane surfaces and a few critical cationic residues on the proteins. Also, the molecular location of these critical cationic residues is species- and enzyme class-specific, despite the highly homologous tertiary structures of these enzymes, and coincides with that of prominent cationic patches seen by surface electrostatic potential calculations (Scott et al., 1994).

Human secretory class IIa PLA_2 (hIIa-PLA_2) has unique structural and functional properties. This enzyme is syn-

[†] This work was supported by grants from National Institutes of Health (GM52598 and GM53987 to W.C. and HL36235 to M.H.G.) and a Biomedical Science Grant from the Arthritis Foundation (W.C.).

* Corresponding authors. W.C.: Tel 312-996-4883; Fax 312-996-0431; email wcho@uic.edu. M.H.G.: Tel 206-543-7142; Fax 206-685-8665; email. gelb@chem.washington.edu.

[‡] University of Illinois at Chicago.

[§] University of Washington.

[∥] University of Southampton.

[⊗] Abstract published in *Advance ACS Abstracts,* October 15, 1997.

[1] Abbreviations: BLPG, 1,2-bis[12-(lipoyloxy)dodecanoyl]-*sn*-glycero-3-phosphoglycerol; BSA, fatty acid-free bovine serum albumin; DMPM, 1,2-dimyristoyl-*sn*-glycero-3-phosphomethanol; HEPES, *N*-(2-hydroxyethyl)piperazine-*N*′-2-ethanesulfonic acid; hIIa-PLA_2, human secretory class IIa phospholipase A_2; IBS, interfacial binding surface; PLA_2, phospholipase A_2; pyrene-PE, 1-hexadecanoyl-2-(1-pyrenedecanoyl)-*sn*-glycero-3-phosphoethanolamine; pyrene-PG, 1-hexadecanoyl-2-(1-pyrenedecanoyl)-*sn*-glycero-3-phosphoglycerol.

S0006-2960(97)01200-2 CCC: $14.00

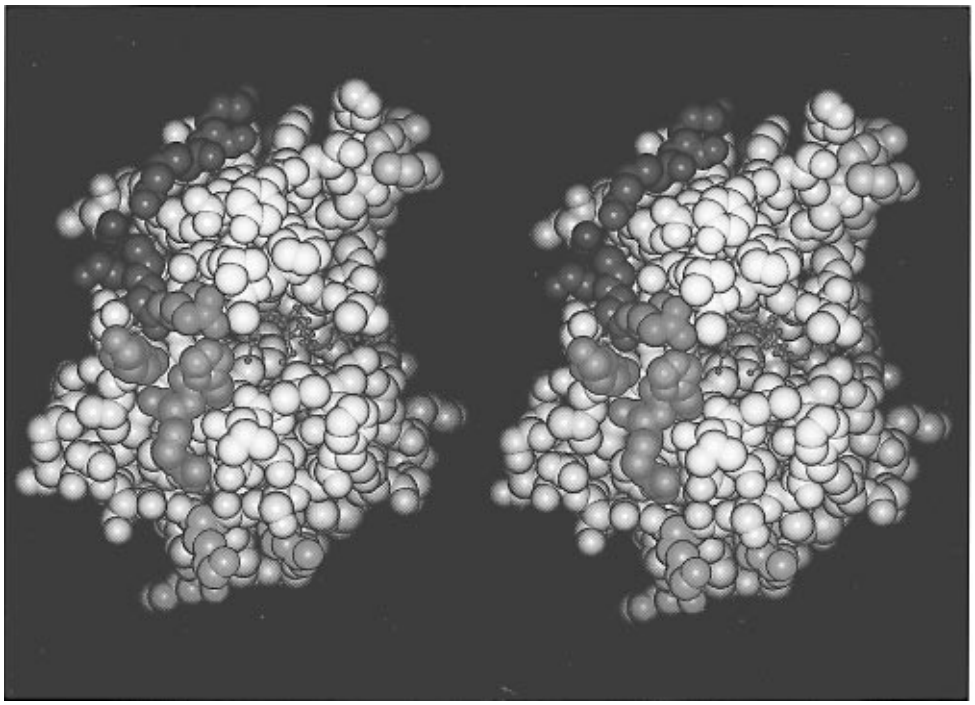

FIGURE 1: Stereo diagram of hIIa-PLA_2 in space-filling representation. The enzyme is oriented with its putative IBS pointing toward the viewer. A short-chain phospholipid analogue inhibitor is shown in light green with its *sn*-1 and *sn*-2 alkyl chains pointing toward the viewer. The inhibitor is bound in the active-site slot, which extends all the way through the globular protein. Residues on the putative IBS are colored as follows: (1) Clusters of cationic residues are as follows: H6/R7/K10 cluster, red; K16/K110/K115 cluster, rust; R34/K124/R127 cluster, orange; K74/K87/R92 cluster, pink; K38/K116 cluster, purple. (2) Hydrophobic residues are in yellow: L2, V3, A19, L20, F24, V31, F70, and Y119. (3) The only anionic residue on the putative IBS is E17, shown in cyan.

thesized and secreted by a variety of cells including platelets (Kramer et al., 1989), neutrophils (Wright et al., 1990), and mast cells (Murakami et al., 1992). Because of its presence in inflammatory fluids, tissue exudates, and serum, hIIa-PLA_2 has been implicated in inflammatory responses including the liberation of arachidonate from cell membranes for the biosynthesis of eicosanoids (Dennis, 1994; Kramer et al., 1989; Kudo et al., 1993, Weiss et al., 1991). The factors that allow the action of hIIa-PLA_2 on certain cells but not on others are not understood. Thus, it is important to understand at the molecular level how hIIa-PLA_2 binds to synthetic and cellular membranes. The crystal structure and surface electrostatic potential calculation of hIIa-PLA_2 have shown that this highly cationic protein contains an unusually large number of prominent cationic patches on its molecular surface, some of which lie on the putative IBS (Figure 1). This is in contrast to bovine pancreatic PLA_2 and *A. p. piscivorus* PLA_2, which display only a limited number of such patches (Han et al., 1997). It has been shown that hIIa-PLA_2 has exceptionally high affinity for anionic surfaces (Bayburt et al., 1993; Dua & Cho, 1994; Kim et al., 1997; Snitko et al., 1997), including anionic phospholipid membranes, heparin and its derivatives, and anionic proteins (Weiss et al., 1994), which may be important for its physiological functions. To identify the amino acid residues that are essential for binding of hIIa-PLA_2 to anionic interfaces, we have performed extensive site-directed mutagenesis of this protein. Herein, we report the results of kinetic and binding studies of the action of hIIa-PLA_2 mutants on anionic phospholipid liposomes.

MATERIALS AND METHODS

Materials. 1-Hexadecanoyl-2-(1-pyrenedecanoyl)-*sn*-glycero-3-phosphoethanolamine (pyrene-PE) and -phosphoglycerol (pyrene-PG) are from Molecular Probes (Eugene, OR). 1,2-Bis[12-(lipoyloxy)dodecanoyl]-*sn*-glycero-3-phosphoglycerol (BLPG) was synthesized as described (Wu & Cho, 1993). Triton X-100 is from Pierce (Rockford, IL). Large unilamellar liposomes of BLPG were prepared by multiple extrusions of a phospholipid dispersion in 10 mM Tris-HCl buffer (pH 8.4) through a 0.1-μm polycarbonate filter in a Liposofast microextruder (Avestin, Ottawa, Ontario) and then polymerized in the presence of 10 mM dithiothreitol (Wu & Cho, 1994). Phospholipid concentrations were determined by phosphate analysis (Kates, 1986). Nonlipid reagents are from the following sources: fatty acid-free bovine serum albumin (BSA) (Bayer Inc., Kankakee, IL); guanidinium chloride and β-mercaptoethanol (Fisher); restriction enzymes, T4 ligase, and T4 polynucleotide kinase (New England Biolabs, Beverly, MA); isopropyl β-D-thiogalactopyranoside (Boehringer Mannheim Biochemicals, Indianapolis, IN), and oligonucleotides (Integrated DNA Technologies, Coralville, IA). 1,2-Dimyristoyl-*sn*-glycero-3-phosphomethanol (DMPM) was prepared as described (Jain & Gelb, 1991).

Construction of Mutant hIIa-PLA_2 Genes. The synthetic gene for hIIa-PLA_2 (Othman et al., 1994) was subcloned into the pET-21a vector (Novagen, Madison, WI) and the construct was designated as pYS. This synthetic gene carries the Asn to Ala mutation (N1A) at the amino terminus to facilitate the removal of the initiator Met by the endogenous methionine aminopeptidase (Othman et al., 1994). Mutagenesis was performed using a Sculptor *in vitro* mutagenesis kit from Amersham (Arlington Heights, IL) according to the method of Nakamaye and Eckstein (1986) with modifications. In this method, a phagemid DNA prepared from the pYS vector in the presence of helper phage R408 (Promega, Madison, WI) was used as a template for mutagenesis. The oligonucleotides used for the construction

of mutants were 5′ CTT GAT CAT ACG TTC GAA GTT TAC CAG 3′ (H6E), 5′ TAA CTT GAT CAT TTC GTG GAA GTT TAC 3′ (R7E), 5′ GGT GGT TAA CTC GAT CAT ACG GTG 3′ (K10E), 5′ GGT TAA CTC GAT CAT TTC GTG GAA GTT TAC CAG 3′ (R7E/K10E), 5′ AGC AGC TTC TTC ACC GGT GGT TAA 3′ (K16E), 5′ CC AGA GTT AGA GAA TTC GTA AGA CAG GAA TTT 3′ (K74E), 5′ A AGA GTC CTG TTC AGC GCA GGT GAT 3′ (K87E), 5′ GCA CAG CTG AGA TTC GCA AGA GTC CTG 3′ (R92E), 5′ GCA CAG CTG AGA TTC GCA AGA GTC CTG TTC AGC GCA GGT GAT 3′ (K87E/R92E), CTG GTA TTT TTC GTT GTA GGT GGT TTC GTT ACG AGC GAA G (K110E/K115E), CGG GGT **C**GA CCC ATC GCA GTG TTC GTT AGA GTA G (K124E/R127D), GCA ACG **A**TC GGT AGC GTC TTC *T*GG GGA CCC (K38E), and GA GTA GTA **T**TG GTA TTC TTT GTT GTA G (K116E). The underlined bases indicate the location of the charge-reversal mutations, and boldfaced bases indicate the location of silent mutations introduced to eliminate or create a diagnostic restriction site. The single italicized base is a mutation introduced to remove a *Nci*I restriction site, whose presence would interfere with DNA manipulations. Most of the multisite mutations (e.g., K74E/K87E/R92E) were performed sequentially; i.e., the K87E/R92E mutation followed by the K74E mutation. After DNA sequences of entire coding regions of mutants were verified using a Sequenase 2.0 kit (Amersham) or by machine sequencing using a dye terminator cycle sequencing kit (Applied Biosystems), individual recombinant pYS vectors were transformed into *Escherichia coli* strain BL21(DE3) (Novagen) for protein expression.

Bacterial Protein Expression and Purification. N1A-hIIa-PLA_2 and most mutant proteins were expressed in BL21(DE3) harboring corresponding pYS vectors. A 2 L culture of Luria broth containing 100 μg/mL ampicillin was grown at 37 °C, and protein expression was induced by the addition of 1 mM isopropyl β-D-thiogalactopyranoside when the absorbance of the culture at 600 nm reached 0.6−0.8. After cells were incubated for an additional 4 h at 37 °C, they were harvested and frozen at −20 °C. For H6E, K10E, K16E, R7E/K10E, and R7E/K10E/K16E, the yield of protein expression using the pET 21a-based pYS vector was low. To improve expression, each mutant gene was subcloned into the pET-30a vector (Novagen), which carried the kanamycin-resistance gene. For these mutants, BL21(DE3) cells harboring corresponding recombinant pET-30a vectors were grown in 2 L of Luria broth containing 30 μg/mL kanamycin, and the protein expression was induced in the same manner.

The frozen cells were thawed and resuspended in 50 mL of buffer A [50 mM Tris-HCl, pH 8.0, 1 mM EDTA, 50 mM NaCl, and 0.5 mM phenylmethanesulfonyl fluoride (added fresh)] containing 0.4% (v/v) Triton X-100 and 0.4% (w/v) sodium deoxycholate, and the suspension was stirred at 4 °C for 20 min. Sonication was performed on ice using a Sonifier 450 (Branson) in pulse mode for 10 × 15 s. The inclusion body pellet was obtained by centrifugation for 20 min at 12000*g* and at 4 °C. The pellet was resuspended in buffer A containing 0.8% (v/v) Triton X-100 and 0.8% (w/v) sodium deoxycholate, sonicated as described above, and centrifuged. The pellet was resuspended and washed by stirring in 50 mL of buffer A containing 1% (v/v) Triton X-100 for 20 min at room temperature. The pellet was collected by centrifugation as described above, washed in 50 mL of buffer A, and centrifuged. Inclusion bodies were solubilized by stirring overnight at 4 °C in 50 mL of buffer A containing 6 M guanidinium chloride and 5% β-mercaptoethanol. Solubilized protein was obtained by centrifugation at 70000*g* for 40 min at 4 °C. The denatured protein was refolded by dialyzing twice against 4 L of 25 mM Tris-HCl buffer, pH 7.5, containing 5 mM $CaCl_2$, 5 mM L-cysteine, and 0.9 M guanidinium chloride for 48 h at 4 °C. Any precipitate was removed by filtration through a 0.45 μm filter. Guanidinium chloride was removed by dialysis against 2 × 4 L of 25 mM Tris-HCl, pH 8.0. To remove any precipitate, the solution was centrifuged for 20 min at 9000*g* , and the supernatant was filtered through a small (2.5 × 5 cm) Sephadex G-25 column equilibrated with 25 mM HEPES buffer, pH 8.0. The clear solution was loaded onto a Pharmacia CM-Sepharose column (2.5 × 20 cm) equilibrated with 25 mM HEPES buffer, pH 8.0. The column was washed extensively with the same buffer until protein elution ceased, and then the folded protein was eluted with a gradient of NaCl from 0 to 2 M in the same buffer. The protein peak was collected, dialyzed against water, lyophilized, and stored at −20 °C. Purity of proteins was confirmed by SDS−polyacrylamide gel electrophoresis. Protein concentrations were determined by the micro bicinchoninic acid method (Smith et al., 1985) (Pierce, Rockford, IL). The mutants K110E/K115E, R38E/K116E, and K124E/R127D were purified by a slightly modified procedure (Othman et al., 1994).

Kinetic Measurements. hIIa-PLA_2-catalyzed hydrolysis of pyrene-PG (or pyrene-PE)/BLPG (1:99 mol/mol) polymerized mixed liposomes was performed at 37 °C in 2 mL of 10 mM Tris-HCl buffer, pH 7.4, containing 2.5 μM total phospholipids, 2 μM BSA, 0.16 M NaCl, and 10 mM $CaCl_2$. Progress of the reaction was monitored as an increase in fluorescence emission at 378 nm using a Hitachi F4500 fluorescence spectrometer with an excitation wavelength of 345 nm. The spectral bandwidth was set at 5 nm for excitation and at 10 nm for emission. The BLPG molecule has a nominal cross-sectional area of 90 Å^2/molecule when maximally packed at the air−water interface. On the basis of this value and the geometry of liposome of 100 nm diameter, the total number of BLPG in a liposomes is estimated to be ca. 60 000. In all of the kinetic experiments, enzyme concentrations were adjusted to maintain $E_T \geq 10L_T$, where E_T and L_T indicate total enzyme and liposome concentrations ($\approx$ [BLPG]/60 000), respectively. Under this condition, most of the mutants (see Results section) displayed a first-order reaction progress curve. The observed first-order rate constant (k) was determined from nonlinear least-squares analysis of the reaction progress curves using the integrated first-order equation [product] = [total product](1 − $e^{-k\,t}$) (Dua et al., 1995; Wu & Cho, 1993, 1994). For each enzyme, k was linearly proportional to the enzyme concentration over at least a 10-fold concentration range (e.g., 0.1−5 nM for wild type); thus, k was divided by the enzyme concentration to obtain the apparent second-order constant, $k_{cat}*/K_M*$. These equations are fully described in the Results section. For those mutants that bind most weakly to anionic vesicles (e.g., R7E/K10E/K16E), the reaction progress curves are more complex. The curves contain a first-order component together with a zero-order component; i.e., they are well fit by the equation [product] = $A(1 - e^{-k\,t}) + k_0\,t$,

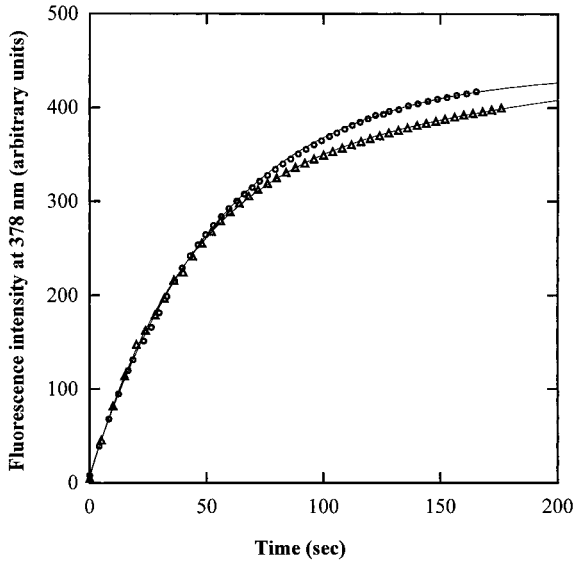

FIGURE 2: Hydrolysis of pyrene-PG/BLPG (1:99) polymerized mixed liposomes by hIIa-PLA_2 (○) and R7E/K10E/K16E (Δ) in 10 mM HEPES buffer, pH 7.4, containing 2 μM BSA, 0.16 M NaCl, and 10 mM $CaCl_2$. Protein concentrations were 0.5 nM for hIIa-PLA_2 and 20 nM for R7E/K10E/K16E, respectively, and the total lipid concentration was 2.5 μM. The solid lines indicate the theoretical curves constructed using the integrate rate equations: [product] = [total product]$(1 - e^{-k\,t})$ for wild type and [product] = $A(1 - e^{-k\,t}) + k_0\,t$ for R7E/K10E/K16E (see Materials and Methods).

where A is a constant and k_0 is a constant describing the zero-order rate (Figure 2).

Hydrolysis of unilamellar vesicles of the anionic phospholipid DMPM was measured using the pH-stat method (Jain & Gelb, 1991). Reaction mixtures contained 4 mL of 1 mM NaCl, 2.5 mM $CaCl_2$, and 5 μg/ml polymyxin B sulfate (Sigma) at pH 8.0 and 21 °C and either 0.6 or 1.2 mg of substrate lipid. Typically 25 ng of wild-type or mutant hIIa-PLA_2 was added to initiate the reaction after the minus enzyme background rate was recorded. Progress curves in the absence of polymyxin B (Figure 4) contained 3 mL of 1 mM NaCl, 0.6 mM $CaCl_2$, and 250 μM DMPM vesicles at pH 8.0 and 21 °C, and reactions were started by the addition of 75 ng of enzyme.

Binding of hIIa-PLA_2 to Sucrose-Loaded Polymerized Liposomes. The binding of wild-type and mutant hIIa-PLA_2 to polymerized liposomes was measured by centrifugation of sucrose-loaded polymerized liposomes as described previously (Lee et al., 1996). Sucrose-loaded BLPG liposomes (400 nm diameter) were prepared in 10 mM Tris-HCl buffer, pH 8.4, containing 0.32 M sucrose and polymerized for 30 h at 37 °C in the presence of 10 mM dithiothreitol. Nonentrapped sucrose molecules were removed by gel-filtration chromatography using a Sephadex G-25 column equilibrated and eluted with 10 mM Tris-HCl buffer, pH 7.4, containing 0.16 M NaCl. For the binding measurements, 50 μM of BLPG polymerized liposomes were incubated with 0.1−2.5 μM of protein solution in 10 mM Tris-HCl buffer, pH 7.4, containing 0.145 M NaCl and 10 mM $CaCl_2$ for 30 min at 37 °C. The mixtures (500 μL each) were then centrifuged for 15 min at 200000*g* and at 37 °C using a Sorvall (Newtown, CT) RCM120EX microultracentrifuge with S120AT3 rotor (Sorvall) to pellet polymerized liposomes. In some experiments, liposomes were doped with 0.1 mol % tritiated 1-palmitoyl-2-oleoyl-*sn*-glycero-3-phosphocholine, and scintillation counting revealed that <3% of liposomes remained in the supernatant after centrifugation. In the absence of liposomes, hIIa-PLA_2 in the range of 10−500 nM retained more than 95% of the activity after centrifugation, thereby precluding the possibility of nonspecific loss of protein to the tube wall during centrifugation. After centrifugation, the concentration of free enzyme ($[E]_f$) in the supernatant was determined by measuring PLA_2 activity toward pyrene-PG/BLPG polymerized mixed liposomes as described above. For each enzyme, the enzyme concentration in which the first-order rate constant is linearly proportional to the enzyme concentration was established and $k_{cat}*/K_M*$ was determined in that range. Typically, this was done by adding 10−400 μl aliquots of the supernatant to 2 mL of 10 mM Tris-HCl buffer, pH 7.4, containing 1:99 pyrene-PG/ BLPG polymerized mixed liposomes (total lipid concentration 2.5 μM), 2 μM BSA, 0.16 M NaCl, and 10 mM $CaCl_2$. The enzyme concentration in this assay mixture was calculated by dividing the first-order rate constant by $k_{cat}*/K_M*$ for each enzyme, and $[E]_f$ was obtained after correcting for dilution. The bound PLA_2 concentration ($[E]_b$) was plotted as a function of $[E]_f$, and values of n and K_d were determined by nonlinear least-squares analysis of the $[E]_b$ vs $[E]_f$ plot using the standard binding equation:

$$[E]_b = ([BLPG]_T/n)/(1 + K_d/[E]_f) \qquad (1)$$

where $[BLPG]_T$ represents total BLPG concentration. Equation 1 assumes that each enzyme binds independently to a site on the interface composed of n phospholipids and with dissociation constant of K_d.

RESULTS

Binding of hIIa-PLA_2 and Mutants to Anionic Polymerized BLPG Liposomes. Cationic patches on the putative IBS of hIIa-PLA_2 (that which surrounds the active-site slot) are shown in Figure 1. To assess the contribution of these cationic residues to interfacial catalysis by hIIa-PLA_2, we made a series of charge-reversal mutants in which a cationic residue(s) is replaced by glutamate (or aspartate). Both single-site and multisite mutations were performed on those cationic residues that are close to the active site slot (e.g., R7E and R7E/K10E/K16E), whereas only multisite mutants were generated for peripheral cationic groups (e.g., K110E/K115E). Since all mutated side chains are solvent-exposed, the mutations were not expected to have significant effects on the structure and stability of the proteins. Indeed, most of mutant proteins were expressed in *E. coli* and subsequently refolded as efficiently as wild type, suggesting comparable thermodynamic stability and a common refolding pathway. Even for those mutant proteins (e.g., K10E; see Materials and Methods) that were expressed in low yield in *E. coli*, their comparable specific enzymatic activities when enzymes are fully bound to vesicles (see Table 1, described later) indicate a lack of any deleterious structural changes. Finally, circular dichroism spectra of wild-type and mutant proteins were essentially indistinguishable (data not shown), again indicating the lack of gross conformational changes of hIIa-PLA_2 due to surface mutations.

The polymerized mixed liposome system allows the systematic and separate analysis of the effect of the mutation of PLA_2 on interfacial binding and on substrate binding in the active site (Dua et al., 1995; Han et al.; 1997, Lee et al.,

Table 1: Kinetic and Membrane-Binding Properties of hIIa-PLA_2 and Mutants[a]

enzymes	pyrene-PE/BLPG polymerized mixed liposomes $k_{cat}*/K_M*$ [b] (M^{-1} s^{-1})	pyrene-PG/BLPG polymerized mixed liposomes $k_{cat}*/K_M*$ [b] (M^{-1} s^{-1})	BLPG polymerized liposomes	
			n	K_d (M)
recombinant wild type	$(2.1 \pm 0.5) \times 10^6$	$(2.3 \pm 0.6) \times 10^7$	25 ± 2	$(1.1 \pm 0.2) \times 10^{-9}$
H6E	$(3.6 \pm 0.8) \times 10^6$	$(1.5 \pm 0.3) \times 10^7$	25 ± 2	$(1.8 \pm 0.3) \times 10^{-9}$
R7E	$(1.1 \pm 0.3) \times 10^6$	$(8 \pm 1) \times 10^6$	23 ± 2	$(2.1 \pm 0.2) \times 10^{-8}$
K10E	$(1.2 \pm 0.3) \times 10^6$	$(9 \pm 2) \times 10^6$	24 ± 2	$(1.2 \pm 0.2) \times 10^{-8}$
R7E/K10E	$(2 \pm 1) \times 10^5$	$(6 \pm 1) \times 10^6$	25 ± 3	$(5 \pm 1) \times 10^{-8}$
R7E/K10E/K16E	$(1.4 \pm 0.5) \times 10^5$	$(1.1 \pm 0.3) \times 10^6$	65 ± 5	$(3.2 \pm 0.8) \times 10^{-7}$
K16E	$(1.3 \pm 0.3) \times 10^6$	$(1.0 \pm 0.3) \times 10^7$	26 ± 2	$(1.1 \pm 0.2) \times 10^{-8}$
K110E/K115E	$(1.5 \pm 0.4) \times 10^6$	$(1.5 \pm 0.3) \times 10^7$	26 ± 3	$(4.1 \pm 0.4) \times 10^{-9}$
K74E	$(2.8 \pm 0.5) \times 10^6$	$(1.4 \pm 0.3) \times 10^7$	25 ± 2	$(2.7 \pm 0.5) \times 10^{-9}$
K87E	$(2.3 \pm 0.5) \times 10^6$	$(2.0 \pm 0.4) \times 10^7$	25 ± 3	$(1.0 \pm 0.2) \times 10^{-9}$
R92E	$(2.6 \pm 0.6) \times 10^6$	$(1.8 \pm 0.3) \times 10^7$	26 ± 3	$(3.6 \pm 0.3) \times 10^{-9}$
K74E/R92E	$(2.6 \pm 0.5) \times 10^6$	$(1.5 \pm 0.3) \times 10^7$	25 ± 4	$(5 \pm 1) \times 10^{-8}$
K74E/K87E/R92E	$(2.8 \pm 0.5) \times 10^6$	$(4 \pm 1) \times 10^6$	25 ± 3	$(2.0 \pm 0.3) \times 10^{-7}$
K38E/K116E	$(1.6 \pm 0.3) \times 10^6$	$(1.3 \pm 0.3) \times 10^7$	25 ± 2	$(1.1 \pm 0.3) \times 10^{-8}$
K124E/R127D	$(1.9 \pm 0.3) \times 10^6$	$(5.8 \pm 0.9) \times 10^6$	28 ± 4	$(5.1 \pm 0.6) \times 10^{-8}$

[a] See Materials and Methods section for experimental conditions and methods to calculate rate constants. [b] Values of $k_{cat}*/K_M*$ represent mean values ± standard errors determined from a minimum of three measurements. Values of n and K_d represent best-fit values ± standard errors determined from nonlinear least-squares analyses of data.

1996). This is based on the unique property of polymerized mixed liposomes, in which phospholipids interacting with the active site of PLA_2 and ones interacting with its IBS are unambiguously distinguished (Wu & Cho, 1993). In this system, the phospholipids that are covalent components of the polymerized matrix cannot dislodge from the interface to enter the enzyme's active site slot. Consequently, matrix phospholipids are not hydrolyzed by PLA_2 bound to matrix liposomes. However, noncovalently linked substrates present in polymerized mixed liposome are PLA_2 substrates and thus enter the active site. If liposomes of nonpolymerized phospholipids are used to measure interfacial enzyme binding, the observed binding is actually a measure of the coupled equilibria:

$$E \overset{\text{vesicle}}{\rightleftharpoons} E^* \overset{S}{\rightleftharpoons} E^*{\cdot}S$$

Here, E is enzyme in the aqueous phase, E* is enzyme at the interface, and E*·S is the interfacial Michaelis complex (substrate in the active site). The second step of the above reaction does not occur with polymerized liposomes, and thus the dissociation equilibrium constant obtained, K_d, reflects only the first step. Monomeric substrates embedded in polymerized mixed liposome bind in the active site without competing for polymerized matrix phospholipids, and thus the variation in the reaction rate with the mole fraction of substrate embedded in the liposome reflects active-site binding and catalysis.

To evaluate the effect of mutations on the putative IBS of hIIa-PLA_2, the binding of wild type and mutants to sucrose-loaded polymerized BLPG liposomes was measured. To promote rapid and quantitative centrifugal pelleting of liposomes, 400-nm diameter polymerized liposomes were used. The binding isotherms for wild type and several mutants are illustrated in Figure 3, and values of n and K_d determined from curve fitting to eq 1 (see Materials and Methods) are listed in Table 1. As reported previously (Bayburt et al., 1993; Kim et al., 1997), hIIa-PLA2 has exceptionally high affinity for anionic vesicles. This in conjunction with the minimum requirement of BLPG concentration for complete pelleting of liposomes ($[BLPG]_T \geq 50\ \mu M$) made it necessary to measure the binding of wild type and tight-binding mutants under the conditions in which a majority of enzyme molecules were bound to BLPG polymerized liposomes (i.e., $[E]_b \gg [E]_f$). Despite this limitation, which hampered accurate determination of K_d

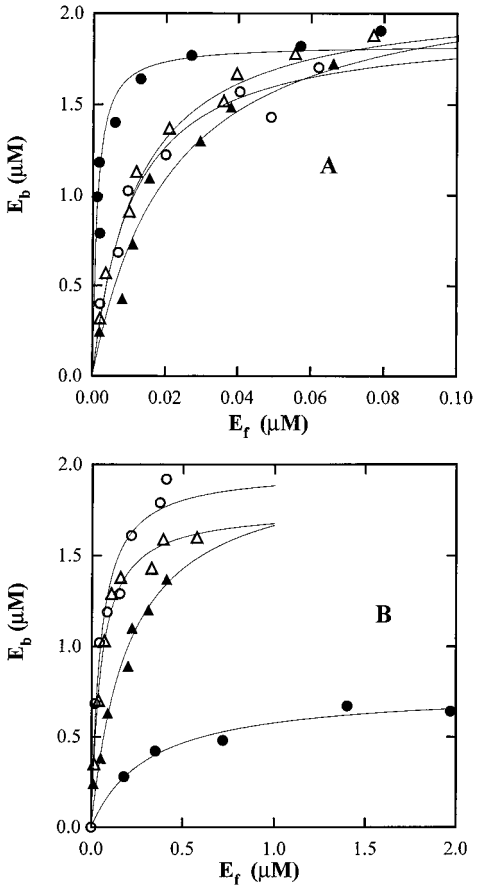

FIGURE 3: Binding isotherms of hIIa-PLA_2 and selected mutants to BLPG polymerized liposomes. Panel A includes wild type (●), R7E (▲), K10E (Δ), and K16E (○) and panel B includes R7E/K10E (○), K124E/R127D (Δ), K74E/K87E/R92E (▲) and R7E/K10E/K16E (●). The bulk BLPG concentration in polymerized liposomes was 50 μM in 10 mM Tris-HCl buffer, pH 7.4, containing 0.16 M NaCl and 10 mM $CaCl_2$. The solid lines indicate theoretical curves constructed using the standard binding equation, $[E]_b = ([BLPG]_T/n)/(1 + K_d/[E]_f)$, with n and K_d values determined from nonlinear least-squares analyses.

values for wild type and tight-binding mutants from curve fitting, theoretical curves constructed using the best-fit values of n and K_d were in good agreement with experimental data. Further, a simulated curve drawn using n and K_d values beyond the range of standard error of each best-fit value noticeably deviated from the experimental data (not shown). Thus, the binding parameters listed in Table 1 allow reasonably accurate comparison of relative membrane-binding affinity of hIIa-PLA_2 and mutants. Finally, with wild type and tight-binding mutants, K_d was measured under conditions of enzyme crowding on liposomes, and because of possible protein−protein interaction, the value obtained might be somewhat different than the K_d obtained under conditions of low liposome coverage. Note that K_d is expressed in terms of molarity of enzyme binding sites composed of n phospholipids. Thus, nK_d is the dissociation constant in terms of molarity of single lipid molecules. Also, the quantity $[BLPG]_T/n$ is the maximum amount of hIIa-PLA_2 that can bind to a given concentration of BLPG polymerized liposomes.

Values of n are virtually identical for all proteins ($n \approx 25$) except R7E/K10E/K16E (see below), which indicates similar binding modes. Note, as defined in this study, n is calculated from $[BLPG]_T$ and not the total amount of lipid in the outer monolayer of vesicles. Since about 60% of the BLPG is in the outer monolayer, multiplying the values of n in Table 1 by 0.6 gives the number of outer layer lipids per enzyme binding site. Values of n are similar to those determined for pancreatic PLA_2 (Dua et al., 1995; Ramirez & Jain, 1991), bee venom PLA_2 (Ghomashchi et al., 1991), and *A. p. piscivorus* PLA_2 (Han et al., 1997). Given the dimensions of secreted PLA_2s and the area occupied by a phospholipid, values of $n = 20-40$ are reasonable. This implies that these enzymes can pack tightly on liposome surfaces. As for K_d, mutant enzymes have a wide range of values (Table 1). Among single-site mutants, R7E, K10E, and K16E showed relatively large decreases (20-, 11- and 10-fold, respectively) in binding to anionic polymerized liposomes, whereas H6E, K74E, K87E, and R92E mutants had modest 2−3-fold drops in binding affinity. This indicates that the three amino-terminal cationic residues that are adjacent to the active-site slot (see Figure 1) make more significant individual contributions to interfacial binding than other more distant residues. The modest effect of His-6 mutation may be due in part to partial deprotonation of this residue at a neutral pH.

Since single-site mutation produces only modest effects on interfacial binding, multisite mutants were prepared (e.g., R7E/K10E and R7E/K10E/K16E). First, the amino-terminal triple-site mutant, R7E/K10E/K16E, shows the lowest binding affinity for BLPG liposomes of all the multisite mutants prepared, binding 290-fold more weakly than wild type. Furthermore, it is the only mutant with an anomalously high n value of 65, implying that it has an altered interfacial binding mode. The double mutant R7E/K10E binds 45-fold more weakly to BLPG liposomes than does wild type. Second, two mutants of the K74/K87/R92 patch, K74E/R92E and K74E/K87E/R92E, bind 40- and 180-fold more weakly than wild type, respectively, to BLPG liposomes. This indicates that the K74/K87/R92 patch, K74 and R92 in particular, also makes a significant contribution to binding of hIIa-PLA_2 to anionic vesicles. Finally, contributions from other cationic patches were assessed by preparing the double-site mutants K110E/K115E, K38E/K116E and K124E/R127D. Compared to wild type, K124E/R127D showed a significant 46-fold increase in K_d, indicating the involvement of these carboxy-terminal residues in supporting enzyme binding to anionic liposomes. K38E/K116E and K110E/K115E showed more modest reductions in binding, 10- and 4-fold, respectively, compared to wild type (Table 1).

Kinetic Studies of hIIa-PLA_2 and Mutants Acting on Anionic Polymerized Mixed Liposomes. Since hIIa-PLA_2 must bind to the interface to hydrolyze phospholipids, mutants with reduced interfacial binding should behave differently than wild-type enzyme in kinetic studies. Initial kinetic studies were carried out with anionic polymerized BLPG liposomes containing small amounts of either pyrene-PG or pyrene-PE as substrate. In these studies, the mole fraction of substrate in the liposome is typically only 0.01. Given that the interfacial Michaelis constant, K_M^*, for hIIa-PLA_2 is about 4 mole fraction for DMPM (Bayburt et al., 1993), at 0.01 mole fraction of pyrene-labeled substrate virtually all of the enzyme will be in the E or E* forms. The interfacial Michaelis−Menten equation for the action of hIIa-PLA_2 under conditions of the mole fraction of substrate much less than K_M^* is given by eq 2 (eq 3 is the integrated form) (Berg et al., 1991):

$$V_0 = \frac{k_{cat}^*}{K_M^*}[S^*][E^*] \tag{2}$$

$$[P]_t = [P]_{max}\left(1 - \exp\left[\frac{k_{cat}^*}{K_M^*}[E]_T t\right]\right) \tag{3}$$

In eqs 2 and 3, bracketed quantities are moles of the species divided by the total reaction volume (aqueous + membrane). V_0 is the initial velocity in molarity product/time, k_{cat}^* is the interfacial turnover number, K_M^* is the interfacial Michaelis constant (in units of moles of substrate in the interface divided by total reaction volume), $[E]_T$ is the concentration of total enzyme, [E*] is the concentration of catalytically productive, interface-bound enzyme, $[P]_t$ is the concentration of product formed at time t, and $[P]_{max}$ is the concentration of product at $t = \infty$. With the conditions used in this study, the enzyme/liposome ratio is larger than 10, and thus the Poisson distribution of the number of enzymes per liposome is very narrow about the expectation value and is not of concern (Berg et al., 1991).

The following mutants displayed first-order reaction progress over the entire reaction: H6E, R7E, K10E, K16E, K110E/K115E, K74E, K87E, R92E, and K38E/K116E. The experimentally measured k_{cat}^*/K_M^* values for these mutants are virtually identical to that for wild type (Table 1). This indicates that these mutants are fully bound to pyrene-PG/BLPG liposomes and that the bound enzyme has the same catalytic efficiency as that of wild type. The former result is expected since the total lipid concentration in these kinetic experiments (2.5 μM) is well above the values of nK_d for these mutants (Table 1). As noted earlier, these results also argue that these mutants are fully folded into a native conformation.

A more complex reaction progress curve was observed with R7E/K10E/K16E, R7E/K10E, K74E/K87E/R92E, K74E/R92E, and K124E/R127D, the mutants that bind weaker to BLPG liposomes. The progress curves were best fit to an

equation involving first-order and zero-order components (Figure 2, see Materials and Methods), although most of the reaction progress still follows the first-order equation. In the presence of 2.5 μM $[BLPG]_T$, a significant fraction of these triple mutants will be in the aqueous phase since their nK_d values $\geq$ 2.5 μM. Also, these mutants almost certainly undergo intervesicular hopping much more rapidly than the tighter binding mutants (confirmed as described later). In the extreme case of weak interfacial binding of enzyme, most vesicles have no bound enzyme and some have at most one bound enzyme. This would impart zero-order kinetics to the reaction progress because before substrate is significantly depleted in an enzyme-containing vesicle, the enzyme travels to a different vesicle that has not become depleted of substrate. Because of the somewhat more complex nature of the reaction progress curves with these mutants, their specific activities are best measured in the presence of sufficiently high vesicle concentrations such that they are fully bound to vesicles. For these studies, DMPM was used as substrate because it is conveniently available in large quantities compared to BLPG. For comparison, the specific activities of wild type and some of the other multisite mutants were measured with the DMPM assay (see Materials and Methods section). In the presence of 250 μM DMPM, the specific activities of the proteins tested expressed as a percentage of the specific activity obtained for wild type are as follows: R7E/K10E, 129%; R7E/K10E/K16E, 92%; K74E/K87E/R92E, 125%; and K124E/R127D, 83%. When the substrate concentration was doubled to 500 μM, the specific activity for wild type increased by only 24%, and the specific activities of the mutants relative to that of wild type are: R7E/K10E, 133%; R7E/K10E/K16E, 99%; K74E/K87E/R92E, 124%; and K124E/R127D, 96%. These results show that with these high lipid concentrations virtually all of the wild-type and mutant enzymes are bound to the interface and that once fully bound the specific activities of the multisite mutants are similar to that for wild type (velocities measured with this DMPM have an error of less than $\pm$10%).

The ability of the mutants to hop among DMPM vesicles was directly investigated as shown in Figure 4. In these experiments, reaction progress curves were obtained for the hydrolysis of DMPM vesicles in the absence of intervesicular phospholipid exchange promoted by polymyxin B (see Materials and Methods). In addition, compared to the experiments shown in Figure 2, much less enzyme was used (75 ng), and thus there are many more vesicles than enzymes. As shown in Figure 4, the reaction rate of wild type decreases considerably well before all of the available substrate is hydrolyzed. As previously shown in detail (Bayburt et al., 1993), this is due to hydrolysis in the scooting mode; i.e., enzyme does not readily dissociate from vesicles. In contrast, R7E/K10E/K16E, which is the weakest vesicle binding mutant, operates in the hopping mode in which the reaction rate does not decrease until most of the vesicles have been hydrolyzed. The double mutant K124E/R127D, which binds with intermediate affinity to anionic vesicles, undergoes more hopping than wild type but less hopping than R7E/K10E/K16E. These results are fully consistent with the vesicle binding data (Table 1).

Kinetic properties of mutant proteins toward BLPG polymerized mixed liposomes containing zwitterionic pyrene-PE substrate rather than anionic pyrene-PG substrate provide additional insights into the role of surface cationic patches in supporting interfacial catalysis by hIIa-PLA_2. Because of the low mole fraction of substrates present in BLPG anionic liposomes (0.01), the physical nature of the interface that drives interfacial enzyme binding should remain unchanged when the substrate is switched from pyrene-PG to pyrene-PE. Wild-type hIIa-PLA_2 catalyzes the hydrolysis of pyrene-PG about 10 times faster than that of pyrene-PE in the BLPG polymerized matrix (Snitko et al., 1997) (Table 1). Most of the mutants displayed comparable relative activity toward pyrene-PE/BLPG versus pyrene-PG/BLPG polymerized mixed liposomes, indicating that the sites of mutation are not involved in substrate binding in the active-site slot (E* to E*·S step). However, the mutants H6E, K74E, K87E, R92E, and K74E/K87E/R92E showed slightly enhanced activity toward pyrene-PE/BLPG polymerized mixed liposomes and hence lower PG/PE ratios than that observed with wild type. Although it does not appear from their surface locations that any of these residues are close enough to the active site to make direct interactions with the bound substrate, mutation of these residues to glutamate may increase the negative electrostatic potential of the active site, which could lead to enhanced binding of pyrene-PE via its cationic amino group. This notion is also consistent with the proximity of these residues to the active-site slot (His-6) and the phospholipid head group binding site (Lys-74, Lys-87, and Arg-92) (Scott & Sigler, 1994).

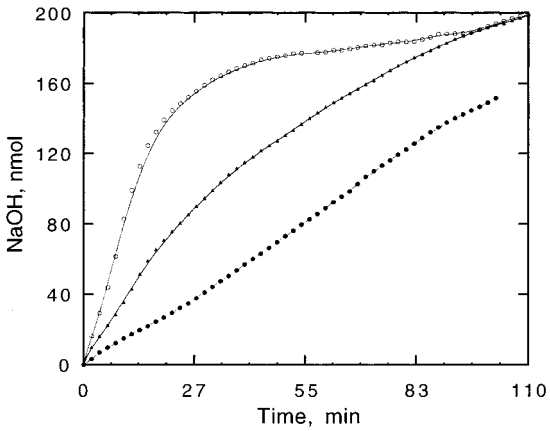

FIGURE 4: DMPM reaction progress curves in the absence of intervesicle phospholipid exchange: wild type (○), K124E/R127D (▲), and R7E/K10E/K16E (●). Reaction mixtures contained 3 mL of 1 mM NaCl, 0.6 mM $CaCl_2$, and 250 μM DMPM vesicles, at pH 8.0 and 21 °C, and reactions were started by the addition of 75 ng of enzyme. The progress curves with the mutants continue until all of the available substrate (60% of the total DMPM that exists in the outer monolayer of vesicles) is hydrolyzed. Late parts of the progress curves for mutants are not shown.

DISCUSSION

Although the secretion of hIIa-PLA_2 from a variety of activated cells that function in inflammatory cascades is well-established, the rules that govern the binding of extracellular hIIa-PLA_2 to specific target cells are not understood at the molecular level. Two possible components of hIIa-PLA_2−cell surface interaction are under investigation. The first stems from *in vitro* studies showing that hIIa-PLA_2 binds much tighter to vesicles of synthetic anionic phospholipids than to zwitterionic phosphatidylcholine vesicles (Bayburt et al., 1993; Kim et al., 1997; Kinkaid & Wilton, 1995). In most mammalian cells, anionic phospholipids segregate

preferentially in the intracellular leaflet of the plasma membrane bilayer, and this leaves the extracellular leaflet with very little net charge (Devaux, 1991). This would disfavor binding of secreted hIIa-PLA_2 to cells. However, some cells, especially platelets, translocate their anionic phospholipids to the outer leaflet after stimulation by a proinflammatory agonist (Comfurius et al., 1994), and this could allow cell surface binding of hIIa-PLA_2. To date, there is no strong evidence for this proposal for hIIa-PLA_2 cell targeting. Inoue and co-workers have suggested a second possible component of hIIa-PLA_2−cell surface binding that involves cell surface proteoglycans such as heparan sulfate (Murakami et al., 1993). Addition of soluble sulfonated glycans such as heparin to cultures of mammalian cells results in the accumulation of secreted hIIa-PLA_2 in the culture medium, possibly because the enzyme is bound to free heparin rather than cell surface heparan sulfate (Suga et al., 1993). Treatment of rat liver-derived BRL-3a cells with heparitinase to cleave cell surface proteoglycans causes a reduction in the levels of eicosanoids induced by secreted hIIa-PLA_2 (Suga et al., 1993). It is not clear if hIIa-PLA_2 is bound simultaneously to cell membranes via its IBS and to cell surface proteoglycans.

A reasonable hypothesis is that cationic residues on the surface of hIIa-PLA_2 allow the enzyme to bind tightly to anionic vesicles and to sulfonated polyglycans such as heparin and heparan sulfate. Studying the role of surface cationic amino acids in promoting the binding of hIIa-PLA_2 to anionic membranes and heparin is a formidable problem because this enzyme has 13 lysine and 10 arginine residues that are scattered over the entire surface of the enzyme. In this study we have focused on cationic residues that lie on or near the putative IBS of hIIa-PLA_2 (Figure 1) and their role in supporting the binding of enzyme to anionic vesicles. Studies with the remaining lysines and arginines on the surface of hIIa-PLA_2 are in progress. Based on proximity to each other, these residues have been cataloged into clusters (Figure 1), and selected lysines and arginines in each cluster have been mutated to anionic residues.

It has been shown that tight binding of hIIa-PLA_2 to anionic phospholipids is driven in part by electrostatic forces (Kim et al., 1997). A major conclusion of the present work is that of all the basic residues on or near the IBS Arg-7, Lys-10, and Lys-16 that are located in the amino-terminal region make most significant individual contributions to the overall electrostatic interactions. Because the value of K_d determined in this study for the interaction of wild-type hIIa-PLA_2 with anionic liposomes is only an upper limit (see Results), one can say that the 290-fold loss in affinity of the triple-site mutant R7E/K10E/K16E to anionic polymerized BLPG liposomes compared to wild type is a lower limit estimate. The finding that the specific activity of R7E/K10E/K16E is comparable to that of wild type toward DMPM under the condition in which all enzymes are bound to liposomes clearly indicates that the mutant is able to bind to liposome surface, albeit less tightly, in a catalytically productive mode. This rules out the possibility that the loss in interfacial binding affinity is due to a significant local or global structural changes. From the equation $\Delta\Delta G^\circ = RT$ ln [K_d for wild type/K_d for R7E/K10E/K16E], one can estimate that the three residues contribute approximately 3.3 kcal/mol at 25 °C to the free energy of binding of hIIa-PLA_2 to anionic liposomes under standard conditions with the concentration of free phospholipid set at 1 M. This energy value compares well with the energy contributions from critical cationic residues of bovine pancreatic PLA_2 and *A. p. piscivorus* PLA_2. Bovine pancreatic PLA_2 contains three prominent cationic residues on its putative IBS (K10, K56, and K116), which contribute 1.2, 2.9, and 2.1 kcal/mol toward interfacial binding, respectively (Dua et al., 1995). Also, K7 and K10 of *A. p. piscivorus* PLA_2 contribute 3.6 kcal/mol in combination (Han et al., 1997). The key importance of R7, K10, and K16 in supporting interfacial binding of hIIa-PLA_2 may be due to the fact that of all the cationic residues on the IBS, these lie closest to the collar of hydrophobic residues that surround the opening of the active-site slot (Figure 1). The other cationic residues lie behind the plane that contacts the surface of hIIa-PLA_2 at the opening to the active-site slot, and thus these residues may be farther from the membrane than R7, K10, and K16. Evidently, other cationic residues on the putative IBS make smaller but significant contributions to the binding of hIIa-PLA_2 to anionic interfaces. Finally, a higher n value for R7E/K10E/K16E suggests that this mutant either binds to liposome surface in a unique, yet catalytically productive, mode or does not pack tightly at the liposome surface due to the protein−protein repulsion.

The surface electrostatic potential calculations of bovine pancreatic PLA_2 and *A. p. piscivorus* PLA_2 (Scott et al., 1994) demonstrate that the locations of the cationic residues most critical for interfacial binding coincide with the locations of the highest cationic potential on their putative IBS. hIIa-PLA_2 has a much larger number of strongly cationic patches on its putative IBS than other secreted PLA_2s and this probably explains why this enzyme binds more tightly to anionic liposomes than pancreatic or *A. p. piscivorus* PLA_2s (Dua et al., 1995; Han et al., 1997). Also, this accounts for relatively high residual binding affinity of R7E/K10E/K16E to anionic liposomes (nK_d for R7E/K10E/K16E is 21 μM, whereas nK_d for the K7E/K10E mutant of *A. p. piscivorus* PLA_2 is > 400 μM). The residual binding affinity of R7E/K10E/K16E comes in part from other cationic residues on the putative IBS, and also from hydrophobic residues that surround the active-site slot (Figure 1); the contribution of the latter remains to be determined. Most notably, two prominent patches, K74/K87/R92 and K124/R127, play significant roles in binding of hIIa-PLA_2 to anionic liposomes. Their estimated energy contributions are 3.1 and 2.4 kcal/mol at 25 °C. In the K74/K87/R92 patch, K74 and R92 are more important than K87, as evidenced by the large effect of the K74E/R92E mutation, and this is consistent with their side-chain orientations (see Figure 1). Note that the effect of the triple-site mutation, R34E/K124E/R127D, on membrane binding was not measured due to the difficulty in expressing this protein. Taken together, electrostatic interactions between these cationic residues on the putative IBS of hIIa-PLA_2 and the anionic interface account in part for the preference of this enzyme for anionic interfaces over zwitterionic ones. However, because the wild type binds too tightly to anionic vesicles to accurately determine the total interfacial binding energy, the exact fraction of this energy that is due to electrostatics cannot be obtained from the data for the charge reversal mutants. These studies pave the way toward a molecular-level understanding of the factors that control the targeting of hIIa-PLA_2 to particular cellular membranes.

REFERENCES

Bayburt, T., Yu, B. Z., Lin, H. K., Browning, J., Jain, M. K., & Gelb, M. H. (1993) *Biochemistry 32*, 573−582.

Berg, O. G., Yu, B. Z., Rogers, J., & Jain, M. K. (1991) *Biochemistry 30*, 7283−7297.

Comfurius, P., Smeets, E. F., Willems, G. M., Bevers, E. M., Zwaal, R. F., Jain, M. K., Yu, B. Z., Rogers, J., Gelb, M. H., Tsai, M. D., Hendrickson, E. K., & Hendrickson, H. S. (1994) *Biochemistry 33*, 10319−10324.

Davidson, F. F., & Dennis, E. A. (1990) *J. Mol. Evol. 31*, 228−238.

Dennis, E. A. (1994) *J. Biol. Chem. 269*, 13057−13060.

Dennis, E. A. (1997) *Trends Biochem. Sci. 22*, 1−2.

Devaux, P. F. (1991) *Biochemistry 30*, 1163−1173.

Dua, R., & Cho, W. (1994) *Eur. J. Biochem. 221*, 481−490.

Dua, R., Wu, S.-K., & Cho, W. (1995) *J. Biol. Chem. 270*, 263−268.

Gelb, M. H., Jain, M. K., Hanel, A. M., & Berg, O. G. (1995) *Annu. Rev. Biochem. 64*, 653−9588.

Ghomashchi, F., Yu, B. Z., Mihelich, E. D., Jain, M. K., & Gelb, M. H. (1991) *Biochemistry 30*, 9559−69.

Han, S.-K., Yoon, E. T., Scott, D. L., Sigler, P. B., & Cho, W. (1997) *J. Biol. Chem. 272*, 3573−3582.

Heinrikson, R. L., Krueger, E. T., & Keim, P. S. (1977) *J. Biol. Chem. 252*, 4913−4921.

Jain, M. K., & Gelb, M. H. (1991) *Methods Enzymol 197*, 112−125.

Kates, M. (1986) *Techniques of Lipidology*, 2nd ed., Elsevier, Amsterdam.

Kim, Y., Lichtenbergova, L., Snitko, Y., & Cho, W. (1997) *Anal. Biochem 250*, 109−116.

Kinkaid, A. R., & Wilton, D. C. (1995) *Biochem J 308*, 507−512.

Kramer, R. M., Hessen, C., Johanson, B., Hayes, G., McGray, P., Chow, E. P., Tizard, R., & Pepinsky, R. B. (1989) *J. Biol. Chem. 264*, 5768−5775.

Kudo, I., Murakami, M., Hara, S., & Inoue, K. (1993) *Biochim. Biophys. Acta 1170*, 217−231.

Lee, B.-I., Yoon, E. T., & Cho, W. (1996) *Biochemistry 35*, 4231−4240.

Mayer, R. J., & Marshall, L. A. (1993) *FASEB J. 7*, 339−348.

Murakami, M., Kudo, I., & Inoue, K. (1993) *J. Biol. Chem. 268*, 839−844.

Murakami, M., Kudo, I., Umeda, M., Matsuzawa, A., Takeda, M., Komada, M., Fujimori, Y., Takahashi, K., & Inoue, K. (1992) *J. Biochem.* (Tokyo) *111*, 175−181.

Nakamaye, K., & Eckstein, F. (1986) *Nucleic Acids Res. 14*, 9679−9698.

Othman, R., Worral, A., & Wilton, D. C. (1994) *Biochem. Soc. Trans. 22*, 317S.

Peters, A. R., Dekker, N., van den Berg, L., Bolens, R., Kaptein, R., Slotboom, A., & de Hass, G. H. (1992) *Biochemistry 31*, 10024−10030.

Ramirez, F., & Jain, M. K. (1991) *Proteins: Struct., Funct., Genet. 9*, 229−239.

Scott, D. L., & Sigler, P. B. (1994) *Adv. Protein Chem. 45*, 53−88.

Scott, D. L., Mandel, A. M., Sigler, P. B., & Honig, B. (1994) *Biophys. J. 67*, 493−504.

Smith, P. K., Krohn, R. I., Hermanson, G. T., Mallia, A. K., Gartner, F. H., Provenzano, M. D., Fujimoto, E. K., Goeke, N. M., Olson, B. J., & Klenk, D. C. (1985) *Anal. Biochem. 150*, 76−85.

Snitko, Y., Yoon, E. T., & Cho, W. (1997) *Biochem. J. 321*, 737−741.

Suga, H., Murakami, M., Kudo, I., & Inoue, K. (1993) *Eur. J. Biochem. 218*, 807−813.

Weiss, J., Wright, G., Bekkers, A. C. A. P. A., van den Bergh, C. J., & Verheij, H. M. (1991) *J. Biol. Chem. 266*, 4162−4167.

Weiss, J., Inada, M., Elsbach, P., & Crowl, R. M. (1994) *J. Biol. Chem. 269*, 26331−26337.

Wright, G. W., Ooi, C. E., Weiss, J., & Elsbach, P. (1990) *J. Biol. Chem 265*, 6675−6681.

Wu, S.-K., & Cho, W. (1993) *Biochemistry 32*, 13902−13908.

Wu, S.-K., & Cho, W. (1994) *Anal. Biochem. 221*, 152−159.

BI971200Z